

$E1$ and $E2$ strength in ^{32}S and ^{34}S observed in α -capture reactions

E. Kuhlmann

*Department of Physics, Stanford University, Stanford, California 94305
and Ruhr Universität Bochum, Bochum, Federal Republic of Germany*

J. R. Calarco, V. K. C. Cheng,* D. G. Mavis, J. R. Hall, and S. S. Hanna

Department of Physics, Stanford University, Stanford, California 94305

(Received 15 January 1979)

Excitation functions and angular distributions of the reactions $^{28,30}\text{Si}(\alpha, \gamma_0)$ were used to study the distribution of $E2$ strength in the energy regions 11–21 MeV of $^{32,34}\text{Si}$, as well as to probe the importance of isospin in the decay of the $E1$ giant resonance in these nuclei. It was found that the $E2$ strength in the (γ, α_0) channel is widely distributed and accounts for about 12% of the energy weighted isoscalar sum rule in each nucleus. Together with the $E2$ strength observed in lower resonances, about 45% of the sum rule is accounted for in ^{32}S and 34% in ^{34}S , where the measurements on the lower resonances are incomplete. The spreading of the $E2$ strength can be attributed to the mixing of np - nh configurations into the basic $1p$ - $1h$ excitations of the $E2$ resonance, and the large $E2$ strength is attributed to the presence of a direct or semidirect component in the (γ, α_0) process. A comparison of the $E1$ strengths in the (γ, α_0) channel of the giant dipole resonances in $^{32,34}\text{S}$ indicates that isospin conservation is important in these reactions. The relative weakness of the $E1$ (γ, α_0) strength in ^{34}S compared to the $E2$ strength is attributed to the relative purity of the $1p$ - $1h$ character of the $E1$ resonance as compared to that of the $E2$ resonance.

NUCLEAR REACTIONS $^{28}\text{Si}(\alpha, \gamma_0)$, $E = 5$ –16 MeV; $^{30}\text{Si}(\alpha, \gamma_0)$, $E = 4$ –15 MeV; measured $\sigma(E, E_\gamma, \Theta_\gamma)$. $^{32,34}\text{S}$ deduced $E1$, $E2$ strengths. Enriched targets.

I. INTRODUCTION

In recent years the α -capture reaction has proved to be an important way to measure the distribution of isoscalar $E2$ strength in light nuclei.^{1–5} This work has shown that, for nuclei with mass $A \leq 40$, the $E2$ strength is distributed broadly up to and including the region of the giant quadrupole resonance (GQR) observed in the inelastic scattering of electrons,⁶ protons,⁷ and other ions.⁸ The (α, γ_0) studies have shown that α decay from the $E2$ resonances is favored over proton decay,⁹ the total $E2$ strength observed in the α -capture reactions being typically 10% of the isoscalar $E2$ sum rule. Recently, it has been demonstrated that the $E2$ strength seen in (α, γ_0) follows fairly well the structure of the strength observed in inelastic excitation in the regions where they overlap.^{10–12}

In this work, we have extended our earlier study⁴ of the reactions $^{20,22}\text{Ne}(\alpha, \gamma_0)$, $^{24,26}\text{Mg}$ to $^{28,30}\text{Si}(\alpha, \gamma_0)$, $^{32,34}\text{S}$. The intensity of the $E1$ strength was found to be much stronger in $^{30}\text{Si}(\alpha, \gamma_0)$, ^{34}S than in the $^{28}\text{Si}(\alpha, \gamma_0)$, ^{32}S reaction, while the $E2$ intensity was comparable in the two reactions. The difference in the $E1$ strengths might be due to the isospin selection rule in a self-conjugate nucleus like ^{32}S , which forbids $E1$ decay between $T = 0$ states. Hence, the $E1$ radiation can occur only through isospin mixing. On the other hand, there is no such selection rule for isoscalar $E2$ decay, so these reactions should be ideal for the study of the $E2$ strength associated with the α_0 channel. The $^{28}\text{Si}(\alpha, \gamma_0)$, ^{32}S reaction has also been

studied by Meyer-Schützmeister *et al.* and by Foote *et al.*³ In Ref. 1 only two angular distributions were measured and no particular emphasis was placed on extraction of the $E2$ strength. However, Ref. 3 dealt directly with $E2$ radiation and an $E2$ strength of 17% of the sum rule was reported to be associated with the α_0 decay. However, the absolute cross sections given in these two papers differ by as much as a factor of three and the present work attempts to resolve this discrepancy.

II. EXPERIMENTAL PROCEDURE AND ANALYSIS

A detailed description of the experiment is given in our earlier work.⁴ An α -particle beam from the Stanford FN tandem Van de Graaff accelerator passed through self-supporting SiO foils and was then stopped 7 m from the target in a shielded dump. For the $^{28}\text{Si}(\alpha, \gamma)$ reaction the ^{28}Si was enriched to 99.84%. The target thickness was measured by comparing the yield of elastically scattered α -particles at $E_\alpha = 5$ MeV and $\Theta = 30^\circ$ with the calculated Rutherford cross section. A thickness of $450 \pm 30 \mu\text{g}/\text{cm}^2$ of SiO was found. A comparison of the observed $^{28}\text{Si}(\alpha, \alpha_0)$ and $^{16}\text{O}(\alpha, \alpha_0)$ yields gave a $\text{Si}:\text{O}$ ratio of 1.00 ± 0.03 for the SiO target. For the $^{30}\text{Si}(\alpha, \gamma)$ reaction the target was $340 \pm 40 \mu\text{g}/\text{cm}^2$ thick and the SiO was enriched in ^{30}Si to 95.55%. Some of the angular distributions were measured with a somewhat thicker target deposited on a Au backing 0.2 mm thick.

The capture γ -rays were detected with the

Stanford 24 cm x 24 cm NaI spectrometer¹³ placed at a distance of 54 cm from the target. The lead collimator of the detector subtended a solid angle of 0.06 sr. Only the ground state transitions were analyzed in both reactions, since the γ -rays populating the first excited states at energies of 2.13 and 2.24 MeV could not always be resolved from lower-energy backgrounds. Additionally, for the $^{28}\text{Si}(\alpha, \gamma_1)^{32}\text{S}$ reaction the γ energy almost coincides with that for the $^{16}\text{O}(\alpha, \gamma_0)^{20}\text{Ne}$ reaction.

The yields of the ground state transitions were obtained by fitting the γ -ray peaks observed in the spectra with a least-square line-shape fitting program. The efficiency of the detector was determined by recording counts accepted and rejected by the annular anticoincidence requirement of the detector¹³ in separate analyzers and was found to be 70%. Small changes in the efficiency due to varying γ -ray energy and varying deadtime in the detector system (amounting to less than 5%) were taken into account.

Excitation functions were measured at $\theta_\gamma = 135^\circ$ and angular distributions at 34, 67.5, 90, 112.5, and 135°, the sequence being measured at least twice. In those cases where the target was on a thick Au backing, spectra were taken at 57° instead of 67.5° in order to reduce the absorption of the γ -rays in the backing of the target which was mounted at an angle of 75° . In these runs the yields obtained at 45° and 57° were corrected for the absorption which was calculated to be the order of 5%. The isotropy

of the target-detector system was measured with a ThC'' source placed at the center of the target chamber and was found to be better than 1%.

The ground state angular distributions were fitted by the expression⁴

$$W(\theta) = (4\pi)^{-1}[(\sigma_{E1} + \sigma_{E2}) - (\sigma_{E1} - 0.7\sigma_{E2})P_2 - 1.71\sigma_{E2}P_4 - 2.68\sqrt{\sigma_{E1}\sigma_{E2}}\cos\delta(P_1 - P_3)]. \quad (1)$$

The cross sections σ_{E1} and σ_{E2} denote the total cross sections for capture through 1^- and 2^+ resonances, respectively, and δ is the phase difference ($\phi_p - \phi_d$) of the respective p and d waves. The P_k are Legendre polynomials. In the analysis the effect of the solid angle of the detector and the correction for the Doppler shift of the radiation were both taken into account.

In order to assess the extracted E1 and isoscalar E2 strengths we employed the following sum rules⁴

$$\int \sigma(E1) dE = 60 \text{ NZA}^{-1} \text{ MeV} \cdot \text{mb}, \quad (2)$$

$$\int \sigma(E2) E_x^{-2} dE = 0.25 \text{ Z}^2 \text{ A}^{-1} \langle R^2 \rangle = 0.22 \text{ Z}^2 \text{ A}^{-1/3} \text{ } \mu\text{b/MeV} \quad (3)$$

with $\langle R^2 \rangle = (3/5)r_0^2 A^{2/3}$ and $r_0 = 1.2 \text{ fm}$.

III. RESULTS

A. The reaction $^{28}\text{Si}(\alpha, \gamma_0)^{32}\text{S}$

The reaction $^{28}\text{Si}(\alpha, \gamma_0)^{32}\text{S}$ ($Q = 6.95 \text{ MeV}$) was studied over the energy range $E_\alpha = 5\text{--}16 \text{ MeV}$. When adjusted for the half thickness of the target (about 100 keV at $E_\alpha = 7.5 \text{ MeV}$) this corresponds to an excitation-energy range from 11.2 to 20.9 MeV. The

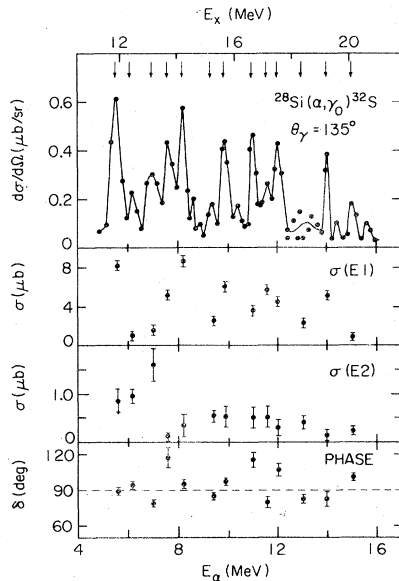


FIG. 1. Top: excitation function at $\theta = 135^\circ$ for the reaction $^{28}\text{Si}(\alpha, \gamma_0)^{32}\text{S}$. The arrows indicate energies at which angular distributions were measured. Middle: the extracted E1 and E2 total cross sections for the (α, γ_0) reaction. Bottom: the E2 phase δ relative to the E1 phase.

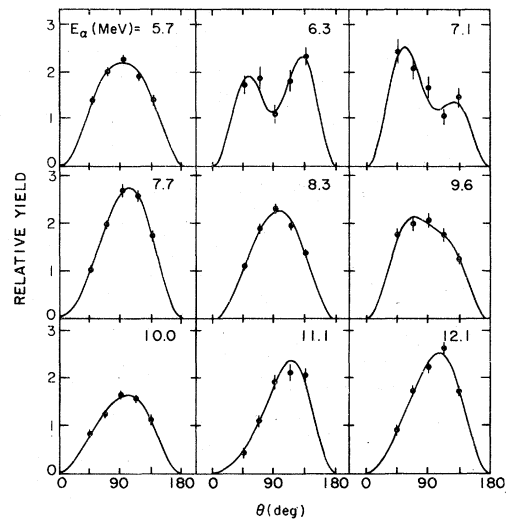


FIG. 2. Typical angular distributions for the reaction $^{28}\text{Si}(\alpha, \gamma_0)^{32}\text{S}$. The solid lines are fits obtained with Eq. (10).

TABLE I. Average values of the cross sections in $^{28}\text{Si}(\alpha, \gamma_0)^{32}\text{S}$ and $^{30}\text{Si}(\alpha, \gamma_0)^{34}\text{S}$.

$^{28}\text{Si}(\alpha, \gamma_0)$			$^{30}\text{Si}(\alpha, \gamma_0)$		
ΔE_x (MeV)	$\bar{\sigma}_{E1}$ (μb)	$\bar{\sigma}_{E2}$ (μb)	ΔE_x (MeV)	$\bar{\sigma}_{E1}$ (μb)	$\bar{\sigma}_{E2}$ (μb)
11.6 - 14.0	4.0	0.87	11.1 - 16.0	22	0.67
14.0 - 20.3	4.3	0.37	16.0 - 19.3	11	0.49
11.6 - 20.3	4.2	0.53	11.1 - 19.3	20	0.62

excitation function at $\theta_\gamma = 135^\circ$ is shown in the upper part of Fig. 1. The average step size was 200 keV. Throughout the energy region studied the differential cross section fluctuates strongly about an average value which decreases from approximately 0.3 $\mu\text{b}/\text{sr}$ at low energy to about 0.1 $\mu\text{b}/\text{sr}$ at high energy.

Angular distributions were measured at the energies indicated by arrows in Fig. 1. A representative set is shown in Fig. 2. The angular distributions were analyzed by means of Eq. (1) and the extracted parameters σ_{E1} , σ_{E2} , and δ are shown in the lower part of Fig. 1. It can be seen that the observed E1 cross section fluctuates about an average value of approximately 4 μb (see Table I). The E2 strength, however, separates into two regions. The first centers around 13 MeV with an average value of about 0.9 μb , whereas the second stretches from 14 MeV to 20 MeV at about 0.4 μb . This is the region where the isoscalar GQR is expected to appear ($63/A^{1/3} = 19.8$ MeV). The phase scatters around $\delta = 90^\circ$, as has already been observed in other α -capture studies. This behavior is discussed below in Section IV.C.

If the α -capture results are converted into (γ, α_0) cross sections by detailed balance, the yield curve can be compared with other photoneuclear reactions such as $^{32}\text{S}(\gamma, p)^{31}\text{P}$, $^{14-16}$ as shown in Fig. 3. Here the (γ, p_0) yield is obtained by detailed balance from the data of Dearnaley et al.¹⁴ The region from $E_x = 14$ -21 MeV is considered to encompass the giant dipole resonance (GDR). The center and the top of Fig. 3 show the $\sigma(\gamma, \alpha_0)$ yield curve and the E2 strength, respectively. The integrated E2 strength observed within the excitation-energy range 11.6 to 20.3 MeV amounts to about 11.6% of the E2 sum rule of Eq. (3), (see Table II). In the same energy region the E1 strength is only 0.9% of the corresponding sum rule. This result will be discussed in Section IV.

Figure 4 gives a comparison of our results with those of Refs. 1 and 3. The 90° excitation function for $^{28}\text{Si}(\alpha, \gamma_0)^{32}\text{S}$ of Ref. 1 is shown in the lower part of Fig. 4 together with the 90° yields obtained from the 135° yield curve and the angular distributions measured in the present experiment. Generally the cross sections reported in Ref. 1 are smaller by a factor of about two.

The upper part of Fig. 4 shows the total E1 cross sections reported in Ref. 3, to-

gether with the corresponding data of the present experiment (Fig. 1). The latter, plotted as triangles, are connected by a dashed line which roughly follows the measured excitation function. Reference 3 does not give a detailed excitation function; instead angular distributions were measured between $E_\alpha = 6.0$ and 11.5 MeV in steps of 0.5 MeV. Some of the E1 cross sections of Ref. 3 agree very well with our data, others however are much larger. The shapes of the angular distributions measured in Ref. 1 (at 8.3 and 10.0 MeV) and in Ref. 3 (at 6.5 MeV) do agree very well with our results (see Fig. 2). The angular distribution measured at 8.3 MeV in Ref. 1 was found to be almost pure dipole in character and a total E1

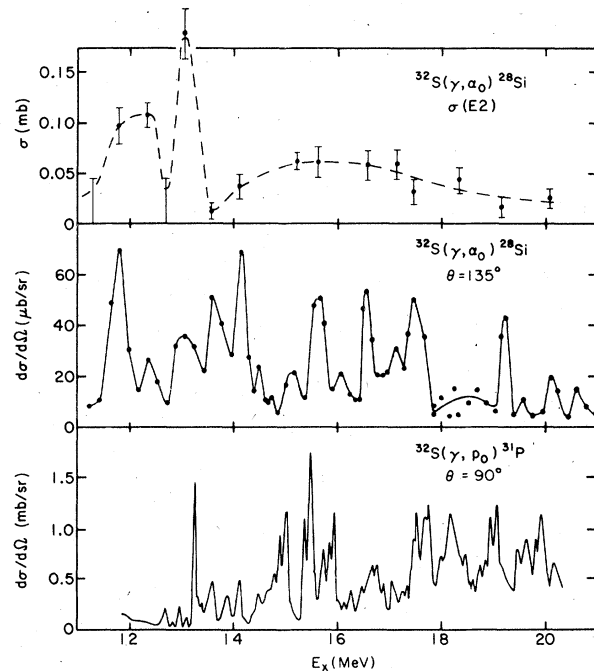


FIG. 3. Top: the total E2 cross section converted by detailed balance to that for $^{32}\text{S}(\gamma, \alpha_0)^{28}\text{Si}$. Middle: the total differential cross section at $\theta = 135^\circ$ converted to $^{32}\text{S}(\gamma, \alpha_0)^{28}\text{Si}$. Bottom: the total differential cross section at $\theta = 90^\circ$ for $^{32}\text{S}(\gamma, p_0)^{31}\text{P}$ obtained by detailed balance from $^{31}\text{P}(p, \gamma_0)^{32}\text{S}$ (Ref. 14).

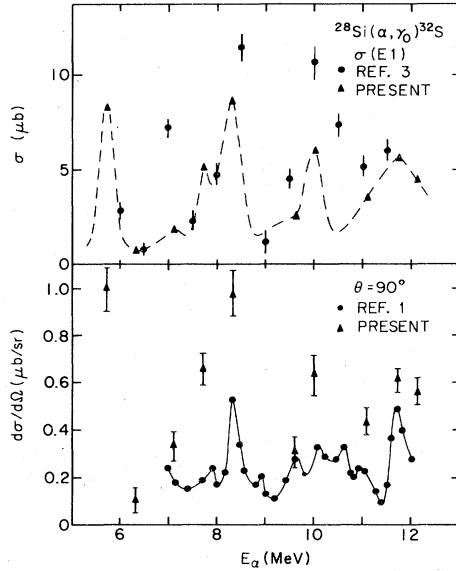


FIG. 4. Top: the E1 cross sections derived from $^{28}\text{Si}(\alpha, \gamma_0)^{32}\text{S}$ in the present work compared with those of Ref. 3. The dashed line is included to guide the eye and follows roughly the (α, γ_0) excitation curve. Bottom: the 90° yields in $^{28}\text{Si}(\alpha, \gamma_0)^{32}\text{S}$ obtained by adjusting the 135° measurements by the measured angular distributions in the present work compared with the 90° yield curve of Ref. 1.

cross section of 4 μb was extracted. This is to be compared with our value of 8.7 μb and the one reported in Ref. 3 of about 12 μb .

We were not able to resolve these strong disagreements. However, the NaI spectrometer¹³ used in these studies has been in operation for several years in the study of capture reactions and has given cross sections in agreement with those obtained in other laboratories including results from (γ, p) studies using bremsstrahlung; the efficiency is therefore well established. Since the cross sections fluctuate strongly with energy, it is possible that small differences in the beam energy can account for some of the discrepancies. Also, the measurement of target thickness or the beam current integration may be at fault. Since the present results were normalized to Ruth-

erford scattering, they will be used in the discussion in Section IV.

B. The reaction $^{30}\text{Si}(\alpha, \gamma_0)^{34}\text{S}$

The reaction $^{30}\text{Si}(\alpha, \gamma_0)^{34}\text{S}$ ($Q = 7.92$ MeV) was studied over the energy range $E_\alpha = 4$ –15 MeV, which corresponds to an excitation-energy range from 11 to 21 MeV. The excitation function taken in about 150 keV steps at $\theta_\gamma = 135^\circ$ is shown in the upper part of Fig. 5. The α -energy scale has been adjusted to the energy loss in the target (about 100 keV for the half thickness at 7.5 MeV). Around $E_x = 12.5$ and 15 MeV two concentrations of strength are visible with peak cross sections up to 2 $\mu\text{b}/\text{sr}$. Above 16 MeV the cross section slowly decreases from an average of about 0.7 $\mu\text{b}/\text{sr}$ at 16 MeV to about 0.1 $\mu\text{b}/\text{sr}$ at 21 MeV.

Angular distributions were taken at those energies marked with arrows in Fig. 5 and analyzed in terms of Eq. (1). In general all the measured angular distributions were similar and displayed a dominant $\sin^2\theta$ dependence which is expected for pure E1 transitions. The extracted parameters are shown in the lower part of Fig. 5. In the region of the main (α, γ_0) yield up to $E_x = 16$ MeV the average relative contribution of the E2 strength underlying the dominant E1 radiation is only about 3% or 0.7 μb (Table I). In the higher energy region there are fewer points which give an average of about 0.6 μb . This is the region where the isoscalar GQR is expected to appear ($63/A^{1/3} = 19$ MeV). The phase δ stays fairly close to 90° reflecting the almost constant shape of the angular distributions. If the yields are converted to (γ, α_0) cross sections by detailed balance, integration of the observed E2 strength over the energy region 11.1 to 19.3 MeV gives a total of 12.6% of the E2 sum rule of Eq. (3), (see Table II). In the same energy region the E1 strength is 3.2% of the corresponding sum rule of Eq. (2).

The conversion of the results in Fig. 5 to the inverse reaction $^{34}\text{S}(\gamma, \alpha_0)^{30}\text{Si}$ by detailed balance preserves the main features of the data and introduces only a mild energy trend into the cross sections. To a very good approximation the results for the inverse reaction can be obtained from the cross section scales given on the right of the figure.

IV. DISCUSSION

The existence of an isoscalar E2 resonance was predicted on quite general grounds

TABLE II. Integrated E1 and E2 strengths in $^{32}\text{S}(\gamma, \alpha_0)^{28}\text{Si}$ and $^{34}\text{S}(\gamma, \alpha_0)^{30}\text{Si}$ and total integrated E2 strengths based on a Hauser-Feshbach calculation.

Nucleus	ΔE_x (MeV)	$\int \sigma(\text{E1}) dE$ (% sum rule)	$\int \sigma(\text{E2})/E^2 dE$ (% sum rule)	ΔE_x (MeV)	$\int \sigma_{\text{tot}}^{\text{CN}}(\text{E2})/E^2 dE$ (% sum rule)
^{32}S	11.6 - 20.3	0.88	11.6	0 - 20.3	≈ 150
^{34}S	11.1 - 19.3	3.2	12.6	0 - 19.3	≈ 370

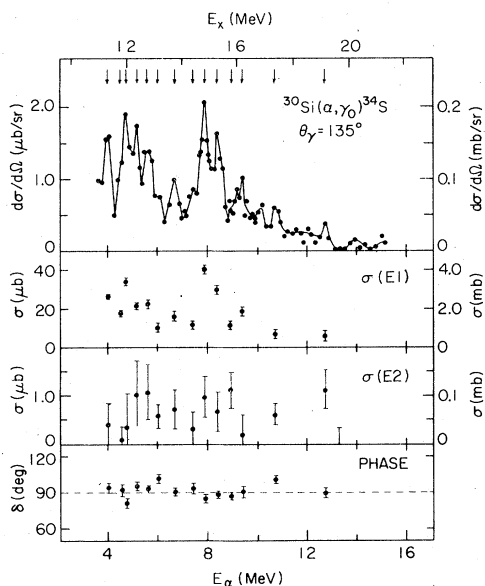


FIG. 5. Top: excitation function at $\theta = 135^\circ$ for the reaction $^{30}\text{Si}(\alpha, \gamma_0)^{34}\text{S}$. The arrows indicate energies at which angular distributions were measured. Middle: the extracted E1 and E2 total cross sections for the (α, γ_0) reaction. Bottom: the E2 phase δ relative to the E1 phase. The ordinate scale given on the right refers to the inverse reaction $^{34}\text{S}(\gamma, \alpha_0)^{30}\text{Si}$.

by Bohr and Mottelson¹⁷ at an excitation energy of $63A^{-1/3}$ MeV. Shell-model calculations^{18, 19} based on lp-1h excitations, carried out for spherical nuclei such as ^{16}O , ^{40}Ca , ^{90}Zr , and ^{208}Pb , also show the GQR at about the same place. Moreover it was predicted that the major part of the E2 strength should fall within a narrow region. In heavy nuclei these predictions are supported by the distributions of E2 strength observed in the various inelastic scattering experiments.⁶⁻⁸

However, in the light nuclei ($A \leq 40$) a somewhat different picture emerges from the observations made by capture reactions.^{9, 20} The observed isoscalar E2 strength in the light nuclei is spread over a large excitation energy region and only part of it appears to be concentrated in the GQR in a region somewhat below the expected location. It is well known that the first excited 2^+ state (in heavy nuclei, as well) carries a substantial amount of E2 strength (up to 20% of the isoscalar E2 sum rule). In the light nuclei additional E2 strength is found in higher excited bound states, as well as in the low-lying resonance levels. Thus, a considerable portion of the E2 sum rule is exhausted below the GQR.

This picture is exemplified by ^{32}S and ^{34}S . The data are summarized in Fig. 6, where the total amount of known E2 strength integrated over 2 MeV wide intervals is plotted as a percent of the E2 sum rule for

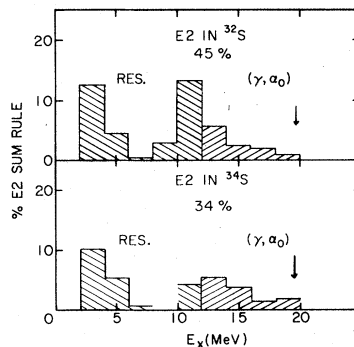


FIG. 6. The E2 strength in ^{32}S and ^{34}S integrated over 2 MeV intervals (in percentage of the isoscalar E2 sum rule) in the bound states and low-lying resonances (Ref. 21) up to $E_x = 12$ MeV and in the α_0 -decay channel (this work) above 12 MeV. The region from 8-10 MeV in ^{34}S is unstudied.

the bound levels,²¹ the low-lying resonance levels,²¹ and the (γ, α_0) process. The arrows mark the predicted center of the GQR at $63A^{-1/3}$ MeV. It can be seen that the observed E2 strength in both cases is spread over the entire energy region and tends to zero at the center of the expected GQR. The observed strength is approximately 45% of the sum rule in ^{32}S and 34% in ^{34}S (in this case there is an appreciable gap in the observations). Concentrations of E2 strength do emerge in these nuclei in a lower and upper region, but it is clear that the picture must be essentially different from that in the heavier nuclei, even when account is taken of the fact that in the upper region only the strength in the α_0 channel is plotted. This spreading of the E2 strength is also observed in the inelastic scattering experiments⁸ which however emphasize the high end of the spectrum (the GQR) since they measure the total E2 strength.

A. The decay of the GQR

We now investigate this question of the other open channels in the decay of the GQR. If it is assumed that the α -capture reaction excites only the compound nuclear (CN) part of the GQR, which in turn decays into channels in a purely statistical way, then it is possible to derive the total absorption cross section for isoscalar E2 radiation $\sigma_{\text{tot}}^{\text{CN}}(\text{E2})$ with the theory of Hauser and Feshbach:

$$\sigma_{\text{tot}}^{\text{CN}}(\text{E2}) = (T_{\alpha_0} / \sum T_i)^{-1} \sigma(\gamma, \alpha_0),$$

where $\sigma(\gamma, \alpha_0)$ is the measured cross section and T_i denotes the transmission coefficient for decay into one of the various p, n, or α channels shown in Fig. 7 for ^{32}S and ^{34}S .

The transmission coefficients T_i were calculated with the computer code ABACUS²² and standard optical model parameters.²³ The ratio $T_{\alpha_0} / \sum T_i$ thus obtained is shown in

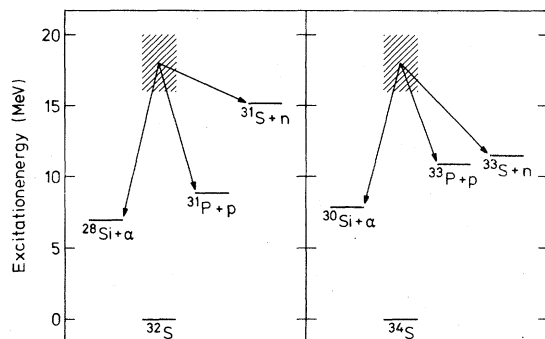


FIG. 7. Energy level diagram for ^{32}S and ^{34}S , showing that many more neutron channels are open for decay to ^{33}S than to ^{31}S .

Fig. 8 as a function of energy for both ^{32}S and ^{34}S . Since the neutron channel for ^{34}S opens at 11.6 MeV (compared to 15.2 MeV for ^{32}S) the ratio is smaller for ^{34}S throughout the energy region investigated. This leads to the interesting results for $\int \sigma_{\text{tot}}^{\text{CN}}(E2)/E^2 dE$ shown in Table II. For ^{32}S the assumption that $\sigma(\gamma, \alpha_0)$ is all compound gives an integrated strength that is about 50% greater than the E2 sum rule, which would suggest the presence of a direct or semidirect yield in the E2 component of $\sigma(\gamma, \alpha_0)$ in ^{32}S . In the case of ^{34}S the assumption of a purely compound process leads to a total strength well over three times the sum rule, which clearly indicates a dominant noncompound component in $\sigma(\gamma, \alpha_0)$ in the E2 strength of ^{34}S .

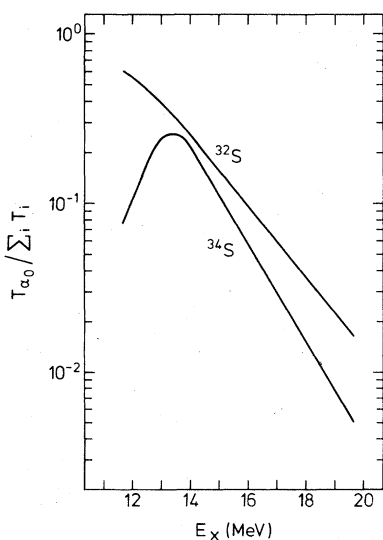


FIG. 8. Percentage of decays in the α_0 channel for ^{32}S and ^{34}S as calculated from Refs. 22 and 23.

B. Configurations of the GQR

It is clear that the distribution of isoscalar E2 strength in light nuclei is quite different than that of the E1 strength in the same mass region. In the latter case, only very little E1 strength is observed below an energy of approximately 15 MeV, the major strength being found in the region of the well known GDR. Thus, the theoretical calculations based on lp-lh excitations of the $1\hbar\omega$ type (Fig. 9) are quite successful in describing the dominant features of the GDR. As mentioned above, one approach to calculations of the GQR has been to simply extend the method of the GDR and use lp-lh excitations of the $2\hbar\omega$ type (Fig. 9). It is not surprising that the general result of these calculations is similar to that for the E1 distribution in placing the major strength in a compact peak at a systematic location in all nuclei. It is obvious that the experimentally observed E2 strength in light nuclei which spreads out over an energy region up to the expected location of the GQR cannot be described by considering only lp-lh excitations.

What then is the cause of the spreading and lowering of the E2 strength in the light nuclei and also of the prominence of the α decay? It is clear that more complex excitations such as 2p-2h (see Fig. 9), 4p-4h, etc. should be included in the calculations. Indeed, calculations of the E2 strength in ^{16}O including 2p-2h excitations²⁴⁻²⁷ show a very pronounced spreading downward of the E2 strength. Such configurations would also favor direct emission of complex particles such as deuterons and alphas, as discussed in Section IV.A above.

The importance of the α -decay channel has also recently been shown in measurements which detect the decay products of the GQR in coincidence with the particles which excite it inelastically.²⁸

C. The phase difference δ

As pointed out above, the phase difference δ scatters about an average value of 90° . This result probably can be attributed to the presence of unresolved fine structure underlying the observed intermediate

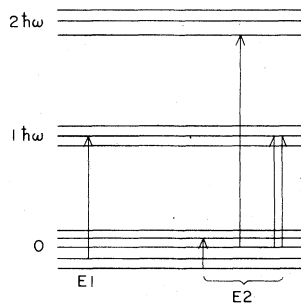


FIG. 9. Schematic diagram of oscillator levels showing possible E1 and E2 transitions in nuclei.

structure. The resulting energy averaging of Eq. (1) then leads to $\langle \cos \delta \rangle \cong 0$. A model of this fine-structure averaging, analyzed with a computer, indicates that the energy averaged values obtained for $\sigma(\text{E1})$ and $\sigma(\text{E2})$ are reliably given in the analysis.

D. Isospin mixing in the GDR

In a self-conjugate nucleus like ^{32}S the GDR has $J^\pi = 1^-$ and $T = 1$, which allows decay into the α_0 channel only if it is mixed into states with $J^\pi = 1^-$ and $T = 0$. On the other hand, there is no such restriction for a non-self-conjugate nucleus like ^{34}S . Thus a comparison of the E1 radiations from the two reactions $^{28}\text{Si}(\alpha, \gamma_0)^{32}\text{S}$ and $^{30}\text{Si}(\alpha, \gamma_0)^{34}\text{S}$ is a very useful way of studying the amount of isospin mixing within the GDR. The results obtained from the cross-section measurements and the angular distributions can be summarized as follows. The average differential cross section of $^{28}\text{Si}(\alpha, \gamma_0)^{32}\text{S}$ is about $0.25 \mu\text{b}/\text{sr}$ (Fig. 1.). The shapes of the angular distributions are mainly dipole in character, but at some energies there is a rather strong contribution from E2 radiation (Fig. 2). The analysis in terms of E1 and E2 amplitudes gives an average ratio of $\bar{\sigma}_{\text{E1}}/\bar{\sigma}_{\text{E2}} \cong 8$ (Table I) which becomes 0.08 in terms of the respective sum rules in the inverse reactions (Table II). On the other hand, the reaction $^{30}\text{Si}(\alpha, \gamma_0)^{34}\text{S}$ has a much larger average cross section of about $1 \mu\text{b}/\text{sr}$ and all the angular distributions display an almost pure dipole character of the form $W(\theta) \sim \sin^2\theta$. The analysis gives an average ratio of $\bar{\sigma}_{\text{E1}}/\bar{\sigma}_{\text{E2}} \cong 32$ (Table I) which becomes 0.25 in terms of the sum rules (Table II). Since

the E2 strength is about the same in both cases, the difference in the two reactions is due to the larger E1 strength in ^{34}S (3.2%) compared to ^{32}S (0.9%) as given in Table II. This result can be attributed to the isospin selection rule given above, and would indicate that isospin is important in these nuclei. A similar result and conclusion was obtained for the $^{24,26}\text{Mg}$ nuclei.⁴

E. Configurations of the GDR

The weakness of the E1 strength in $^{34}\text{S}(\gamma, \alpha_0)^{30}\text{Si}$ (3.2% of the sum rule) compared to the relative E2 strength (12.6% of the sum rule) supports the discussion above on the different character of the GDR and GQR in these nuclei. It was noted that the GQR was spread out and had a relatively large α width which could be explained by strong mixing of np-nh configurations into the basic lp-lh excitations. The GDR, on the other hand, is more compact and has a much smaller α width which is consistent with a purer lp-lh configuration. This picture is supported by the known evidence in the light nuclei. The lp-lh description of the GDR also extends to the heavy nuclei, but as yet the evidence on the GQR is not complete enough to establish its basic character.

This work was supported in part by the National Science Foundation. One of us (E.K.) wishes to acknowledge the support of the Max Kade Foundation for a postdoctoral research fellowship. We wish to thank Jerry Fisher and Scott Wissink for carrying out absolute cross section measurements on these reactions.

*Present address: Institute of Nuclear Science, National Tsinghua University, Hsinchu, Taiwan.

¹L. Meyer-Schützmeister, Z. Vager, R.E. Segel, and P.P. Singh, Nucl. Phys. **A108**, 180 (1968).

²M. Suffert and W. Feldman, Phys. Lett. **24B**, 579 (1967); K.A. Snover, E. G. Adelberger, and D.R. Brown, Phys. Rev. Lett. **32**, 1061 (1974).

³R. B. Watson, D. Branford, J. L. Black, and W. J. Caelli, Nucl. Phys. **A203**, 209 (1973); G. S. Foote, D. Branford, N. Shikazono, and D. C. Weissner, J. Phys. A **7**, L27 (1974).

⁴E. Kuhlmann, E. Ventura, J.R. Calarco, D.G. Mavis, and S. S. Hanna, Phys. Rev. C **11**, 1525 (1975).

⁵R. E. Peschel, J.M. Long, H. D. Shay, and D. A. Bromley, Nucl. Phys. **A232**, 269 (1974).

⁶R. Pitthan and Th. Walcher, Phys. Lett. **36B**, 563 (1971).

⁷M. B. Lewis and F. E. Bertrand, Nucl. Phys. **A196**, 337 (1972).

⁸L. Rutledge and J. Hiebert, Phys. Rev. Lett. **32**, 551 (1974); J. M. Moss, C. M. Rozsa, D. H. Youngblood, and A.D. Bacher, Phys. Rev. Lett. **34**, 748 (1975).

⁹S. S. Hanna, in Proceedings of the International Conference on Nuclear Structure and Spectroscopy, Amsterdam, 1974, edited by H.P. Blok and A. E. Dieperink (Scholar's Press, Amsterdam, 1974), Vol. II, p. 249.

¹⁰D. H. Youngblood, C.M. Rozsa, J. M. Moss, D. R. Brown, and J. D. Bromson, Phys. Rev. C **15**, 1644 (1977).

¹¹F. E. Bertrand, K. van der Borg, A. G. Drentje, M. N. Harakeh, J. van der Plicht, and A. van der Woude, Phys. Rev. Lett. **40**, 635 (1978).

¹²L. Meyer-Schützmeister, R. E. Segel, K. Raghunathan, P.T. Debevec, W. R. Wharton, L. L. Rutledge, and T. R. Ophel, Phys. Rev. C **17**, 56 (1978).

¹³M. Suffert, W. Feldman, J. Mahieux, and S. S. Hanna, Nucl. Instr. Meth. **63**, 1 (1968).

¹⁴G. Dearnaley, D.S. Gemmell, B. W. Hooton, and G. A. Jones, Nucl. Phys. **64**, 177 (1965).

¹⁵W. M. Mason, N. W. Tanner, and G. Kernel, Nucl. Phys. **A138**, 253 (1969).

¹⁶J.R. Calarco, H.F. Glavish, E. Kuhlmann, P.M. Kurjan, and S.S. Hanna, Bull. Am. Phys. Soc. **19**, 496 (1974).

¹⁷A. Bohr and B.R. Mottelson, Nuclear Structure (Benjamin, New York, 1975), Vol. II,

- p. 477.
- ¹⁸S. Krewald and J. Speth, Phys. Lett. 52B, 295 (1974).
- ¹⁹G.F. Bertsch and S.F. Tsai, Physics Reports 18C, 125 (1975).
- ²⁰S. S. Hanna, in Lecture Notes in Physics: Photonuclear Reactions, Erice, 1976, edited by S. Costa and C. Shaerf (Springer-Verlag, Heidelberg, 1977), Vol. I, pp. 275-339.
- ²¹P.M. Endt and C. Van der Leun, Nucl. Phys. A214, 1 (1973).
- ²²E.H. Auerbach, Brookhaven National Laboratory Report No. 6562, 1962 (unpublished).
- ²³R.B. Leachman, P. Fessenden, and W.R. Gibbs, Phys. Rev. C 6, 1240 (1972).
- ²⁴R.J. Philpott and P.P. Szydlick Phys. Rev. 153, 1039 (1967).
- ²⁵W. Knüpfer and M.G. Huber, Z. Physik, A 276, 99 (1976).
- ²⁶J.S. Dehesa, S. Krewald, J. Speth, and A. Faessler, Phys. Rev. C 15, 1858 (1977).
- ²⁷T. Hoshino and A. Arima, Phys. Rev. Lett. 37, 266 (1976).
- ²⁸K.T. Knöpfle, G.J. Wagner, P. Paul, H. Breuer, C. Mayer-Böricke, M. Rogge, and P. Turek, Phys. Lett. 74B, 191 (1978).